Proc. 2nd Saudi Sci. Conf.,Fac. Sci., KAU, 15-17 March 2004, ***Part II,*** pp. 203-210 (2005 A.D./1425 A.H.)

EBIC Contrast of Extended Defects: Theory, Experiment and Monte Carlo Simulations

M. LEDRA [1] and N. TABET [2]
[1] *Institute of Physics, University of Biskra, Algeria.*
[2] *Surface Science Laboratory, Physics Department, KFUPM, Saudi Arabia*
Email: natabet@kfupm.edu.sa

ABSTRACT. The Electron Beam Induced Current (EBIC) technique has been widely used to image the recombination activity of various extended defects including dislocations and grain bonndaries in semiconductors. In this paper, we deseribe a Moute Carlo algorithm that we have developed to simulate the EBIC eontrast at a defect of arbitrary shape loeated underneath the Schottky contact. Then we discuss the results that we have obtained for a disloeation perpendieular to the surface.

Keywords: Dislocatious. EBIC. Monte Carlo Simulations. Recombination contrast.

1. Introduction

Extended defects such as dislocations, grain boundaries and preeipitates affect to a large extent the electrical properties of semiconductors. In general, they contribute to the carrier seattering and recombination. They reduce the mobility and the lifetime of the majority and minority carriers respectively. As a result, the performance of semieonduetor devices such as solar cells, photodetectors and bipolar transistors are drastically affected by the presence of these defects. Electron Beam Induced Current (EBIC) technique has been extensively nsed to observe the recombination activity of various defects (Holt, 1989), and (Tabet 1991). The recombination of the carriers at the defects leads to a current loss and the formation of a dark contrast. Fig. 1 gives an example of EBIC image obtained on a Au/Ge Schottky contact. The dark lines are activc defects..

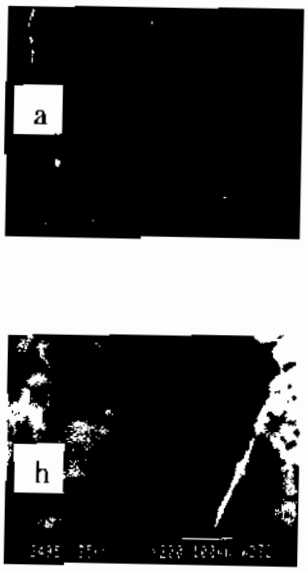

Fig. 1. SEM image (a) and EBIC image of active defects (dark lines) in Gc (b).

The first comprehensive model of the EBIC contrast of defects has been published by Donolato (Donolato, 1978). Analytical solutions have been obtained by considering a simplified description of the defects. For instance, dislocations and grain boundaries have been considered as linear and planar defects respectively, Donolato (1978a, b), Pasemann (1982) and Marek (1983).

Monte Carlo simulation is an alternative method that can provide a more realistic analysis of the recombination contrast of extended defects Akamatsu (1981) and Joy (1986). We present in this paper the algorithm that we have developed to simulate the electrons trajectories in the solid target, the energy dissipation and the distribution of point-like carrier generation sources. The EBIC contrast of the dislocation is obtained by simulating the random diffusion and recombination of the generated carriers.

2. Monte Carlo algorithm

2.1 *Electron trajectories and energy dissipation:*

First, the electron trajectories are simulated using an approach similar to that developed by Murata *et al.* (1971) and Murata, (1974). Figure 2, shows the two scattering angles, θ and ϕ, of an electron. The angle ϕ can be selected randomly between 0 and 2π as follows:

$$\phi = P_1 * 2\pi$$

where R_1 is a random number uniformely distributed between 0 and 1.

Assuming that significant angular deviations result only from elastic scattering events, the scattering angle θ is calculated using the following formula: (Newbury, 1986)

$$\cos\theta = 1 - \frac{2\alpha R_2}{1 + \alpha - R_2}$$

where R_2 is a random number between 0 and 1, and α is the screening parameter given by :

$$\alpha = \frac{0.0034 Z^{\frac{2}{3}}}{E} \quad (\text{E in keV})$$

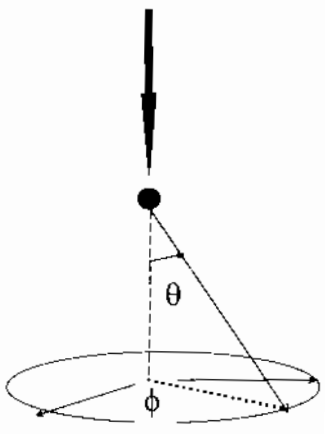

Scattering angles

Fig.2. Scattering angles

The step length is determined from the total scattering mean free path λ_{Tot} by means of the following equation: Adesida *et al.* (1980), Kang-Yoon *et al.* (1990),

$$S = -\lambda_{Tot} \ln R_3$$

where R_3 is a random number between 0 and 1.

The total scattering mean free path λ_{Tot} is given by

$$\frac{1}{\lambda_{Tot}} = \frac{1}{\lambda_{el}} + \frac{1}{\lambda_{in}}$$

λ_{el} is the elastic mean free path given by (Newbury,1986):

$$\lambda_{el} = \frac{A}{\sigma_{el} N_A \rho} \text{ (cm/events)}$$

Where N_A is the Avogadro's number, ρ is the density and A is the atomic weight of the target, and σ_{el} is the elastic cross section given by :

$$\sigma_{el} = \frac{Z^2 e^4}{4E^2} \frac{\pi}{\alpha(1+\alpha)}$$

λ_{in} is the inelastic mean free path given by

$$\lambda_{in} = \frac{A}{\sigma_{in} N_A \rho}$$

Where σ_{in} is the total inelastic scattering cross section given by: (Fontaine, 1978) :

$$\frac{\sigma_{in}}{\sigma_{el}} \cong \frac{20}{Z}$$

Figure 3 shows the electron trajectories of 100 electrons of 20keV energy incident on a Germanium target.

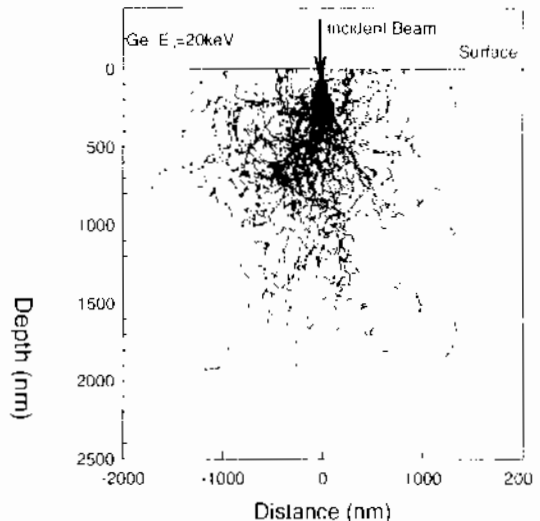

Fig. 3. Electron trajectories in Ge, E0=20keV.

The energy dissipation is simulated by assuming that the electron loses energy continuously. The expression of Bethe (Bishop,1965)

$$\frac{dE}{dS} = -7.85\times10^{4}\left(\frac{\rho Z}{AE}\right)\ln\left(\frac{2E}{J}\right)$$

(keV/cm)

Where E is the electron energy, Z is the atomic number, A is the atomic weight of the target, S is the distance along the trajectory, ρ is the density and J is the mean ionization potential given by: (Newbury,1986):

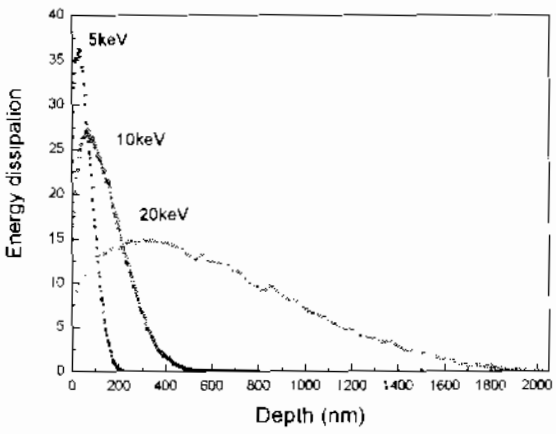

Fig. 4. Energy dissipation versus depth at different incident beam energies in Ge.

$$J = \left(9.76Z + 58.5Z^{\,0.19}\right)\times10^{-3}\ \text{(keV)}$$

The energy loss ΔE along a segment of path of length S is approximated as :

$$\frac{E_{p+1} - E_p}{S} = -\left|\frac{dE}{dS}\right|_{E_p}$$

Figure 4 shows the profiles of the energy loss per unit depth, $\frac{\Delta E_A}{\Delta z}$, in a germanium target, as a function of depth z for several incident energies E_0.

3. Simulation of the dislocation contrast

The generation function g (r) was obtained in the form of a three dimensional distribution of pointlike sources S_i whose coordinates (x_i,y_i,z_i) were taken as the middle of the path between the successive collisions. The number of carrier generated at S_i was taken proportional to the energy loss during the step i. The dislocation was considered as a cylinder of radius r_D perpendicular to the surface.

The depletion region of the Schottky contact was neglected. The carrier lifetime within the dislocation (τ_D) is smaller than in its surrounding bulk (τ_B). The random diffusion/recombination of the carriers emitted from each pointlike source was simulated by considering successive small steps of Δt duration. The time interval Δt was taken as a small fraction of the carrier lifetime in the bulk or in the defect depending on the location of the carrier. The carrier diffuses along a distance $\Delta S = (D\Delta t)^{1/2}$ where D is the diffusion constant of the carrier. The constant D was given the same value in the bulk and inside the

defect as it is usually done in the analytical models. We have considered values of Δt that give a step length ΔS much smaller than the radius of the dislocation.

A carrier was considered as collected if it reaches the surfacc (taken as the edge of the Schottky contact. The collection probability of the carrier generated at a pointlike source S_i was calculated as the ratio of the collected carriers to the number of carriers gencrated at S_i. The programs was run for two positions of the incident electron beam. The first position, far away from the dislocation, gives the current in absence of defect (I_0). The second position gives the current I collected when thc incident electron beam is on thc top of the dislocation . The maximum contrast was obtained as the ratio:

$$C_{max} = \frac{I_0 - I}{I_0} = 1 - \frac{I}{I_0}$$

We have also computed the current collected far away from the dislocation (I_0) by multiplying the number of carriers generated at the depth z_i by the colleetion probability $\exp(-z_i/L_B)$ and summing over all sources S_i. The comparison of the two values of I_0 allowed us to test the reliability of our algorithm in simulating the collected current as the theoretical model provides the exact value of the current in absence of dcfect. The results show a difference less than 5% between simulated and theoretical values (Table 1).

Table 1. Comparison of theoretical and simulated current in absence of defect, L_B=1μm.

E_0(kcV)	7	10	15	20
Io- Theory	0.914	0.8518	0.7215	0.5758
Io -Simulations	0.9136	0.8317	0.7247	0.5576

We have carried out computations to establish thc variation of the contrast upon differcnt parameters such as the primary beam energy, E_0 , the dislocation radius, r_D, the minority carrier diffusion length within the dislocation cylinder, $L_D=(D\tau_D)^{1/2}$ and within the bulk , $L_B=(D\,\tau_B)^{1/2}$. The activity of dislocation is usually described by the parameter γ called the recombination strcngth and given by :

$$\gamma = \frac{\pi r_D^2}{D}\left(\frac{1}{\tau_D} - \frac{1}{\tau_B}\right)$$

Figure 5 shows the variation of the maximum contrast upon thc incident beam cnergy for a dislocation of recombination strength equal $\gamma = 0.1\pi$.

We have also reported on the figurc the theoretical curves obtained by Donolato (1991) for two different values of the dislocation radius: 100nm and 300nm corresponding to the same parameter $\gamma = 0.1\pi$. .

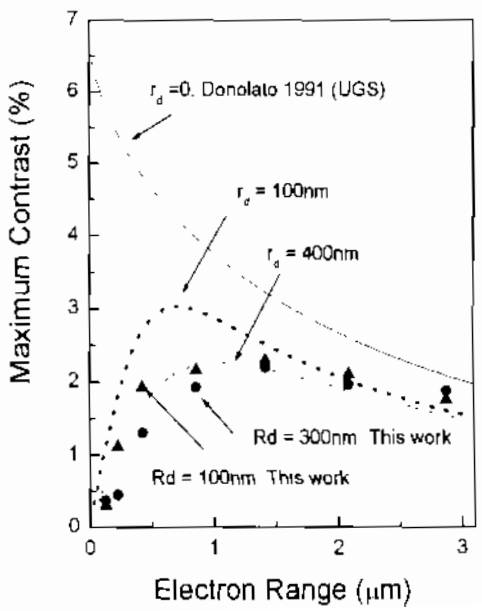

Figures 5 shows also the variation of the contrast versus the electron range for a dislocation considered as a linear defect (zero radius) and having the same recombination strength $\gamma = 0.1\pi$. This curve was obtained by Donolato (1991) using a first order approximation for a uniform Generation Sphere (UGS). One can observe a good agreement between the theoretical curves and the simulated one for a non zero-radius dislocation. The contrast vanishes at low energy beam as predicted by both Pasmann (1991) and Donolato (1991). Notice that Pasmann used a uniform generation sphere while Donolato used a spherical symmetrical Gaussian Generation. The difference between the simulated values of the contrast and those obtained with Donolato's model ranges from 5% and 28%. It should be pointed out that the values of the contrast obtained by Donolato using the first order approximation are 20-30% higher than those obtained by the Pasmann. This observation points out clearly the sensitivity of the EBIC contrast to the generation function and shows that our algorithm provides values of the contrast that are in excellent agreement with the theoretical computations.

Fig. 5. Variation of the EBIC versus the primary electron range. The dots are the simulated values.

4. Conclusion

We have developed a Monte Carlo algorithm that simulates the incident electron trajectories and the three dimensional generation of carriers in solids. We have used the algorithm to simulate the diffusion-recombination process of carriers in semiconductors and to calculate the EBIC contrast of a surface-perpendicular dislocation. The contrast dependence upon the energy of the incident beam was found in excellent agreement with that given by theoretical models.

Acknowledgment

N.T would like to thank King Fahd University of Petroleum and Minerals for its support.

References

Akamatsu, B. and **Henoc, J.P.,** *J. Appl. Phys.*, **52,** (1981) 7245.
Adesida, I., Shimizu, R. and **Everhart, T.E.,** *J. Appl. Phys.*, **51**(11), (1980) 5962
Bishop, H.E., *Proc. Phys. Soc.*, **85,** (1965) 855.
Donolato, C. (1978,a): *Optik,* **52,** (1978/79), p. 19.
Donolato, C. (1978,b): *Appl. Phys. Lett.*, **34**(1), (1979) 80.
Donolato, C. (1991): *J. Appl. Phys.*, **70**(12) (1991), p. 7657.
Fontaine, G. (1978): *«Microanalyse et Microscopie Electronique à Balayage»,* Proceeding de l'école d'été de St-Martin-d'Hères, Les éditions de Physique, ORSAY (France) (1978) 39.
Holt, D.B. and **Joy, D.C.** (1989): *'SEM Microcaracterization of Semiconductors',* Academic Press, London, 1989.

Joy, D.C. (1986): *J. of Microscopy,* **143,** Pt 3 (1986), p. 233.

Kang-Yoon Lee, Guang-Sup Cho and **Duk-In Choi,** (1990): *J. Appl. Phys.,* **67**(12), (1990) 7560.

Marek, J. (1983): *J. Appl. Phys.,* **53,** (1983), p. 1454.

Murata, K., Matsukawa, T. and **Shimizu, R.** (1971): *Jap. J. Appl. Phys.,* **10**(6), (1971) 678.

Murata, K. (1974): *J. Appl. Phys.,* **45**(9), (1974) 4110.

Newbury, D.E., Joy, D.C., Echlin, P., Fiori, C.E. and **Goldstein, J.I.** (1986): *«Advanced Seanning Electron Microseopy and X-Ray Microanaysis».* Plenum Press, New York, (1986).

Pasemann, L. (1991): *J. Appl. Phys.,* **69**(9), (1991) 6387.

Pasemann, L. (1982): *Phys. Stat. Sol.,* **(a) 70,** (1982), p. 197.

Tabet, N. (1991) in *'Structure and Property Relationships for Interfaces',* **Water, J.L., King, A.H.** and **Tangri, K.** (Editors), *ASM Publication,* (1991), p. 361.

تباين العيوب الممتدة الناتج عن التيار المحرض بحزمة إلكترونية النظرية و التجربة والمحاكاة العددية

محمد لضرع [١] و نوار ثابت [٢]

[١]قسم الفيزياء، جامعة بسكرة، الجزائر

[٢]مختبر علم السطوح، قسم الفيزياء، جامعة الملك فهد للبترول و المعادن الظهران، المملكة العربية السعودية

المستخلص. استعملت تقنية التيار المحرض بحزمة إلكترونية استعمالا واسعا لتصوير حركة الالتحام الشحني في العيوب الممتدة مثل التفككات والحدود الحبيبية في شبه الموصلات. نصف في هذا البحث تكوين التباين في صور (EBIC) لعيوب ممتدة في شبه الموصلات. نعرض النتائج التجريبية التي حصلنا عليها وهي تخص الحدود الحبيبية في الجرمانيوم. نناقش التحليل النظري للتباين وحدود صلاحية النماذج المتداولة. نعرض طريقة محاكاة منتي كارلو التي طورناها لحساب تباين EBIC لعيب ذي شكل غير محدد. تعتمد الطريقة على محاكاة المسارات الإلكترونية داخل الشبه موصل والطاقة المبددة التي تحدد توليد حاملات الشحنات تحت القصف الإلكتروني. يتم حساب تباين EBIC المتعلق بعيب ذي شكل خاص عن طريق محاكاة الانتشار العشوائي للحاملات الشحنية المولدة. نعتبر العيب الممتد كمنطقة حيث تكون مدة حياة حاملات الشحنة فيها أقل من قيمتها في المنطقة المحيطة بالعيب. نعرض النتائج المحصل عليها المتعلقة بتفكك عمودي على توصيل شوطكي. نناقش أثر مختلف عوامل المحاكاة مثل طول المرحلة وعدد حاملات الشحنة على استقرار قيم التباين. أخيرا، نقوم بتحليل تغير التباين بدلالة طاقة الإلكترونات الساقطة وقوة الالتحام الشحني للتفكك.